BIOCHEMISTRY
including biophysical chemistry & molecular biology

Article

pubs.acs.org/biochemistry

Analysis of Conformational Changes in the DNA Junction-Resolving Enzyme T7 Endonuclease I on Binding a Four-Way Junction Using EPR

Alasdair D. J. Freeman,[†,§] Richard Ward,[†,§] Hassane El Mkami,[‡] David M. J. Lilley,[†] and David G. Norman*[,†]

[†]Nucleic Acid Structure Research Group, College of Life Sciences, University of Dundee, Dow Street, Dundee DD1 5EH, U.K.
[‡]School of Physics and Astronomy, University of St. Andrews, St. Andrews FE2 4KM, U.K.

Supporting Information

ABSTRACT: The four-way (Holliday) DNA junction is the central intermediate in homologous recombination. It is ultimately resolved into two nicked-duplex species by the action of a junction-resolving enzyme. These enzymes are highly selective for the structure of branched DNA, yet as a class these proteins impose significant distortion on their target junctions. Bacteriophage T7 endonuclease I selectively binds and cleaves DNA four-way junctions. The protein is an extremely stable dimer, comprising two globular domains joined by a β-strand bridge with each active site including amino acids from both polypeptides. The crystal structure of endonuclease I has been solved both as free protein and in complex with a DNA junction, showing that the protein, as well as the junction, becomes distorted on binding. We have therefore used site-specific spin-labeling in conjunction with EPR distance measurements to analyze induced fit in the binding of endonuclease I to a DNA four-way junction. The results support the change in protein structure as it binds to the junction. In addition, we have examined the structure of wild type and catalytically inactive mutants alone and in complex with DNA. We demonstrate the presence of hitherto undefined metastable conformational states within endonuclease I, showing how these states can be influenced by DNA-junction binding or mutations within the active sites. In addition, we demonstrate a previously unobserved instability in the N-terminal α1-helix upon active site mutation. These studies reveal that structural changes in both DNA and protein occur in the action of this junction-resolving enzyme.

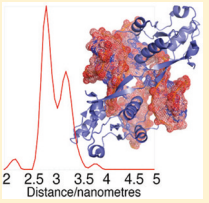

Recognition and manipulation of the DNA four-way (Holliday) junction are central to the process of homologous recombination,[1−4] which is important in the generation of genetic diversity and to some DNA damage repair processes. Resolution of the recombination intermediate requires recognition and cleavage of the four-way DNA junction in a structure-selective manner.[5] Phage T7 endonuclease I is a homodimer composed of 149 amino acids per monomer.[6−8] The protein binds the four-way DNA junction with a dissociation constant of ~1 nM[9] and cleaves on either side of the junction. Although recognition is structural rather than based on any sequence preference, endonuclease I significantly distorts the DNA structure. Several crystallographic structures have defined the basic structures of endonuclease I on its own[10,11] and in complex with a small four-way DNA junction.[12] It has been proposed that some flexibility exists in the endonuclease I dimer and that a small but significant conformational change takes place on binding to a four-way DNA junction.[12] It has also been shown that upon binding to a four-way DNA junction the resultant cleavage is sequential rather than simultaneous.[13] Residues from both polypeptides contribute to each active site of endonuclease I (Asp55, Glu55, and Lys67 from monomer A and Glu20 from monomer B) and two metal ions are present in each.[14] Endonuclease I has been shown to be catalytically active in the presence of magnesium, manganese, iron(II), or cobalt(II) ions but inactive with calcium ions, although calcium still binds in the same location as these other ions within the active site.[14] The DNA is held in an intimate embrace by a combination of interactions with basic residues of the protein and direct contacts between the DNA backbone and the active site metal ions. The protein forms two long perpendicular DNA-binding channels that match the disposition of the helical arms in the bound junction. This requires that the structure of the DNA junction is severely altered on binding. It is therefore of considerable interest to explore the structures of free and bound DNA and enzyme in solution.

In this current study, we have employed site-directed spin-labeling (SDSL)[15] and pulsed electron−electron double resonance (PELDOR or DEER) spectroscopy[16−20] to investigate spin-labeled four-way DNA junction binding to wild-type (wt) endonuclease I and spin-labeled endonuclease I (wt and cleavage inactive mutants) alone and bound to a four-way DNA junction. PELDOR is a powerful tool for measuring long-range distances between unpaired electrons, in the range 2−8 nm or longer.[21,22] PELDOR can be applied to chemically identical spin-label pairs; thus, this method is ideally suited to protein systems that are homodimeric. The protein in this study has

Received: August 1, 2011
Revised: September 29, 2011
Published: October 18, 2011

been labeled with (1-oxyl-2,2,5,5-tetramethylpyrroline-3-methyl)methanethiosulfonate spin-labels (MTSSL) attached to cysteine residues at specific positions in the protein. The quality of the data obtained has allowed accurate description of both the modal distances and the distance distributions between symmetrically labeled protein dimers.

EXPERIMENTAL PROCEDURES

Preparation of Endonuclease I. Endonuclease I was expressed in *E. coli* BL21(DE3)pLysS at 37 °C to an absorbance of A_{600} = 0.6 from a pET19endo I vector prepared as described previously.[26] After induction with 0.1 mM IPTG and further incubation at 30 °C for 4 h the cells were harvested by centrifugation. Cells were resuspended in five volumes of PS buffer (50 mM sodium phosphate (pH 8), 1 M NaCl) supplemented with the complete protease inhibitor cocktail (Roche) and lysed by sonication. The lysates were cleared by centrifugation at 45000*g* for 30 min and applied to a nickel-loaded HisTrap HP (GE Healthcare). The N-terminal oligo-histidine-tagged protein was eluted using a 10−500 mM imidazole gradient in PS buffer. The histidine tag was removed from endonuclease I by digestion with TEV protease. The pure protein was extensively dialyzed against 50 mM Tris-HCl (pH 8), 100 mM NaCl, 1 mM dithiothreitol. Protein concentrations were measured optically, using an absorption coefficient of 49500 M^{-1} cm^{-1} at 280 nm for a dimer of endonuclease I.

Proteins were subjected to anion exchange chromatography on Sephadex SP (GE Healthcare) to remove excess reducing agent prior to labeling with MTSSL. Before chromatography, 20 mM dithiothrietol was added to the sample to reduce cysteine residues fully. Spin-labeling was carried out for 1 h at 4 °C with a 10-fold excess of MTSSL and a protein concentration of 20−100 μM dimer. Unreacted MTSSL was removed by dialysis against water, and protein samples were lyophilized prior to use. Derivatization of endonuclease I by MTSSL was verified by measurement of mass using MALDI.

DNA Synthesis and Spin-Labeling. Oligodeoxynucleotides were synthesized by phosphoramidite chemistry on an Applied Biosystems 394 DNA/RNA synthesizer.[29,30] DNA oligomers were synthesized on a 1 μmol scale by using standard reaction cycles, except that a longer coupling time (600 s) was used for the 2′-aminouridine phosphoramidite (Chemgenes). In our hands, yields for 2′-amino U addition were always low. After release from the solid support, the dimethoxytrityl (DMT) oligonucleotides were deprotected with concentrated ammonium hydroxide for 16 h at room temperature. The DNA oligomers were applied to an ACE10 C-18 reversed-phase HPLC column and eluted with a gradient of acetonitrile against 100 mM triethylammonium acetate buffer (pH 7.0). Fractions containing the DMT-protected DNA oligonucleotides were pooled, and an equal volume of 100% acetic acid was added. The solution was left at room temperature for 25 min, after which it was dried overnight under vacuum. The dried sample was resuspended in water, ethanol precipitated, centrifuged, and resuspended in 70 mM boric acid buffer (pH 8.7) to a final concentration of ∼2 mM.

The preparation of both the spin-labeling reagent and the labeling reaction itself was carried out essentially as previously described,[31,32] except that the 4-isocyanato-TEMPO was dissolved in acetonitrile. The reaction solution contained DNA (stock concentration 2 mM) dissolved in 50% (v/v) 70 mM boric acid buffer (pH 8.7), 30% (v/v) formamide and 10% (v/v) dimethylformamide, which was cooled to 0 °C by means of an ice bath. 10% (v/v) 4-isocyanato-TEMPO (stock concentration 25 mg/100 μL acetonitrile) was added to the reaction solution. After 1 h, the reaction mixture was extracted three times with twice the reaction volume of dichloromethane. The aqueous layer was applied to an ACE 5 C18 reverse-phase column and eluted with a gradient of acetonitrile against 100 mM triethylammonium acetate buffer (pH 7.0). The fractions containing DNA were dried overnight under vacuum. The dried samples were pooled, resuspended in water, and ethanol precipitated.

DNA junctions were purified by gel electrophoresis in polyacrylamide under nondenaturing conditions and eluted from excised gel fragments by diffusion into buffer. The DNA was ethanol precipitated before being resuspended in D_2O.

Sample Preparation for EPR. Spin-labeled, lyophilized protein was resuspended in 50 μL of D_2O containing 20 mM HEPES (pH 7.5) buffer, 100 mM NaCl, and 20 mM $CaCl_2$ and then diluted with an equal volume of d_8-glycerol (50 μL) to make a final volume of 100 μL. Samples were typically 100 μM in concentration. When required, DNA junction was added as a concentrated solution in D_2O directly to the protein, prior to the addition of glycerol.

Activity Testing of Mutant and Spin-Labeled Mutant Endonuclease I. Each sample studied by EPR was tested for DNA junction binding affinity and junction cleavage activity. Experimental conditions are described in the Supporting Information.

PELDOR Experiment. Experiments were performed using a Bruker ELEXSYS E580 spectrometer operating at X-band with a dielectric ring resonator and a Bruker 400U second microwave source unit. All measurements were made at 50 K with an overcoupled resonator giving a Q factor of ∼100. The video bandwidth was set to 20 MHz. The four-pulse, dead-time free PELDOR sequence was used, with the pump pulse frequency positioned at the center of the nitroxide spectrum. The frequency of the observer pulses was increased by 80 MHz relative to the pump position. The observer sequence used a 32 ns π-pulse; the pump π-pulse was typically 16 ns. The experiment repetition time was 4 ms, and the number of shots at each time point was 50. The number of time points and scans used were varied for each sample (see Supporting Information Table 1), but sufficient data were collected to obtain a reasonable signal-to-noise; i.e., the oscillation was more significant than the apparent noise.

PELDOR Data Analysis. Data were analyzed using the DeerAnalysis 2006 software package.[33] In brief, the dipolar coupling evolution data were corrected for background echo decay using a homogeneous three-dimensional spin distribution. The starting time for the background fit was optimized to give the best fit Pake pattern in the Fourier transformed data and the lowest root-mean-square deviation background fit. Tikhonov regularization was then used to simulate time trace data that gave rise to distance distributions, $P(r)$, of peak width depending on the regularization factor, alpha. The alpha term used was judged by reference to a calculated L-curve. The L curve is a parametric plot that compares smoothness of the distance distribution to the mean-square deviation. The most appropriate alpha term to be used is at the inflection of the L curve, since this provides the best compromise between smoothness (artifact suppression) and fit to the experimental data.

Spin-Label Ensemble Generation. Molecular dynamics was carried out using XPLOR-NIH[34] to generate ensembles of

spin-label conformers.[35] Coordinates were mutated within XPLOR to replace required positions with spin-label-derivatized cysteine. Non-Cα backbone positions were restrained by a harmonic function to initial positions, and the unrestrained atoms were allowed to move under molecular dynamics (without an electrostatic potential) at a temperature of 400 K. After a period of equilibration, structures were taken at regular intervals and the distances between MTSSL nitrogen atoms were calculated, collected in groups (40 bins between 2 and 8 nm) and displayed as interpolated lines.

RESULTS

Conformational Change of a DNA Junction on Binding of Endonuclease I Observed by EPR. Endonuclease I is a structure-selective DNA binding protein. Crystal structures of endonuclease I free and bound to a DNA junction indicate that there is a large change in DNA conformation upon binding to endonuclease I. An unbound four-way DNA junction will exist as an equilibrium between an open square structure and the right-handed stacked conformation, with the latter stabilized in the presence of divalent cations. Single molecule FRET indicated that a junction of the type used here will exist in a dynamic equilibrium between two stacking conformers, biased about 4:1 to one of them.[23] The crystal structure of endonuclease I, bound to a small four-way DNA junction, shows the DNA junction exists in a left-handed, nearly perpendicular, stacked conformation.[12] To validate the conditions used in the EPR distance measurement studies and to confirm the stoichiometry of the interaction, we used a spin-labeled cruciform junction with the central sequence of junction 3. This has two short arms terminated by hairpin loops that completely force the complex into a single form[9] as exploited in the crystallographic study (see Supporting Information Figure S1). This species was used to follow the binding process as a function of DNA to protein ratio. Figure 1

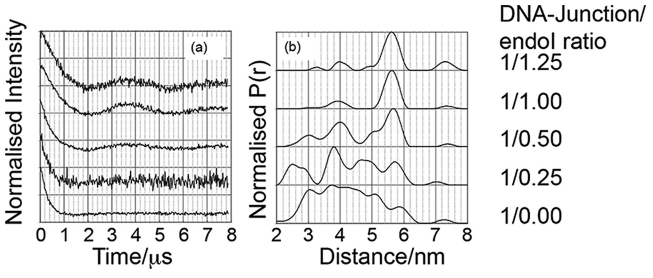

Figure 1. EPR data for spin-labeled four-way DNA junction as a function of endonuclease I concentration. The four-way DNA junction carried spin-labels at Y33 and Z34. In this experiment endonuclease I was unlabeled. (a) Background corrected PELDOR data. (b) Tikhonov-derived distance distribution.

shows a titration of a spin-labeled four-way DNA junction, labeled on different arms at positions Y33 and Z34 (see Supporting Information Figure S2), with an increasing proportion of wild-type (wt) endonuclease I. In the absence of protein, spin-labeled DNA alone demonstrates a dipolar coupling, as evidenced by the oscillation depth of the background-corrected data (Figure 1). The raw data contain no apparent persistent dipolar oscillation, and Tikhonov regularization to determine the spin−spin distances leads to a very broad and convoluted distance envelope. The nature of the data precludes detailed deconvolution of spin−spin distances from the resultant distance envelope; however, it is apparent that the overall result indicates the presence of a number of DNA conformations. Sequential addition of endonuclease I to the labeled junction results in the monotonous emergence of a single, well-defined distance distribution centered on 56 Å. At an approximate ratio of 1:1 junction to protein dimer, the transformation was observed to be essentially complete. The distance distribution observed correlated well with the distance predicted from the crystal structure of the complex. Although a small amount of DNA junction appeared to remain unbound at a DNA−protein ratio of 1:1, increasing the protein−DNA ratio to 125% did not reduce this apparent unbound fraction. The radical ordering of the DNA structure upon being bound by endonuclease I is in marked contrast to the minor structural changes seen in the protein, which is discussed in the following section.

In order to study the structure of endonuclease I both free and in complex with four-way DNA junction, we created a number of mutations in the protein to introduce single cysteine residues on each monomer. Derivatization of these single modified proteins using MTSSL, thereby placing the R1 side chain at these positions (see Supporting Information Figure S3), has allowed us to examine distances between selected regions of the polypeptides in the presence or absence of four-way DNA junction, each reporting on a specific aspect of the structure. These vectors have also been measured in the presence or absence of active site mutations that have previously been studied and in one case crystallized. The labeling sites used were, T51R1, S96R1, and K22R1, with or without the active site mutations K67A and D55A (Figure 2).

Distance Measurements on Spin-Labeled Endonuclease I, T51C. T51 was chosen as an initial labeling site in order to examine the conformational flexibility of the protein alone and in comparison to the four-way DNA junction complex. The vector joining the T51 residues runs approximately along the β-bridge connecting the two domains of the dimeric protein. The raw PELDOR data for T51R1 show three clear oscillations (Figure 3(a)i), indicating that an accurate description of both the distance and the distance distribution between the spins would be possible. The oscillations in the PELDOR data had not fully decayed by the end point so that although background correction might be expected to be reasonable, a long distance truncation artifact was anticipated. The distance distribution obtained by Tikhonov regularization (Figure 3(a)iii) gave three peaks at 29.6 Å (2.3), 33.6 Å (2.6), and 38 Å (2.1); the widths of the peaks at half-height are given in parentheses (alpha fitting factors are shown in Supporting Information Figure S4). The small, long-distance peak (~38 Å) is likely to be the expected data-truncation artifact. Analysis of structure 1MOI, by molecular dynamics, gave a predicted median spin−spin distance of 33 Å. Although molecular dynamics predicted the main distances, it did not indicate the split distance distribution observed in the EPR-derived distance distributions. The use of an R1 rotamer library approach[25] gave results that, while grossly similar to the molecular dynamics results, were more complicated and difficult to interpret.

While a split distribution from one observation alone might indicate restriction of the local spin-label environment leading to two major conformations, subsequent observations make this unlikely and a more probable explanation would be that the signal is derived from two different protein backbone conformations. In spite of the observation of two major distances for T51R1, the distributions are well-defined and the

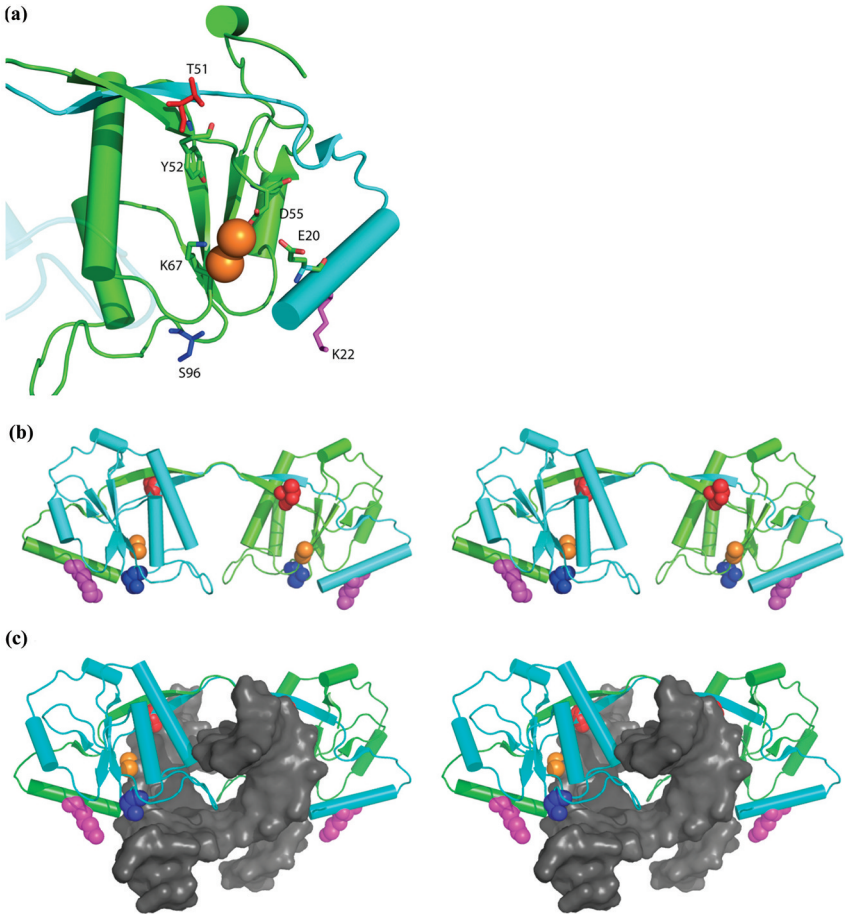

Figure 2. Structural views of endonuclease I. (a) The active site of endonuclease I. Critical active site residues (D55, K67, and E20) are shown as sticks. Y52 is also shown to highlight its presence close to the active site. (b) Parallel-eye stereo view of endonuclease I alone (PDB code 1M0I). One polypeptide is colored cyan and the other light green. (c) Stereo view of endonuclease I bound to a four-way DNA junction (PDB code 2PFJ). Spin-labeling sites shown as sticks (a) or spheres (b, c) and colored as follows: T51 (red), S96 (blue), and K22 (magenta). Bound metal ions are shown as orange spheres. α-Helices, β-sheets, and loop regions are represented by cylinders, arrows, and tubes, respectively. Graphic images were generated using PyMOL.[24]

peak widths are indicative of two distinct conformational states. The major distance of 33.6 Å is in good agreement with the crystal-structure (PDB structure 1MOI), indicating that this is therefore representative of the solution structure, with the β-sheet bridge connecting the two globular parts of the structure being relatively inflexible. The nature of the shorter distance (29.6 Å) is unknown but represents a relatively small yet significant difference from the crystal structures.

Distance Measurements on Spin-Labeled Endonuclease I, T51R1 Junction Complex. On addition of four-way DNA junction to endonuclease I T51R1, a shift of approximately −1 Å in the two main distance distributions was observed (Figure 3(b)iii). The relative intensities of the two major peaks were also observed to change, on DNA binding, with the shorter distance becoming significantly more intense than the longer one. Comparison of the crystal structures without and with DNA shows only small changes in overall conformation, and thus the −1 Å change observed by EPR is not surprising.

It should be noted that the quality of the PELDOR data is such that the major distances and distance distributions should be accurate. Furthermore, the position of T51R1 in the complex is unlikely to be directly influenced by the backbone of the bound DNA. Simulations by molecular dynamics show an R1 distribution that is not significantly occluded by the position of the DNA backbone.

Distance Measurements on Spin-Labeled Endonuclease I, T51R1-K67A. As part of this study, data were gathered on mutations previously shown to inactivate the nucleolytic activity of endonuclease I while retaining junction binding. One such mutation that has been extensively studied is K67A, which lies at the heart of the active site (Figure 2(c)) but remote from T51. When examined by PELDOR, T51R1-K67A endonuclease I in the absence of DNA showed no change in the two major distances that were observed in the wild-type protein, but there was a significant change in the intensity ratios (Figure 3(c)). These are quite similar to those observed when wild-type protein was bound to a four-way DNA junction (Figure 3(b)). K67A has no direct contact with the T51 site and so would not be expected to have a direct influence on the local dynamics of T51R1. This result thus reinforces our opinion that the split distance distribution seen for T51R1 is not due to local steric conditions around the spin-label but rather is due to a more global structural dimorphism. K67A is however intimately involved with the active site of endonuclease I, and it would seem possible that mutation of K67 might change the structure of the active site, into which extends the neighbor of T51, i.e., Y52 (see Figure 2(c)). Thus,

dx.doi.org/10.1021/bi2011898 | *Biochemistry* 2011, 50, 9963–9972

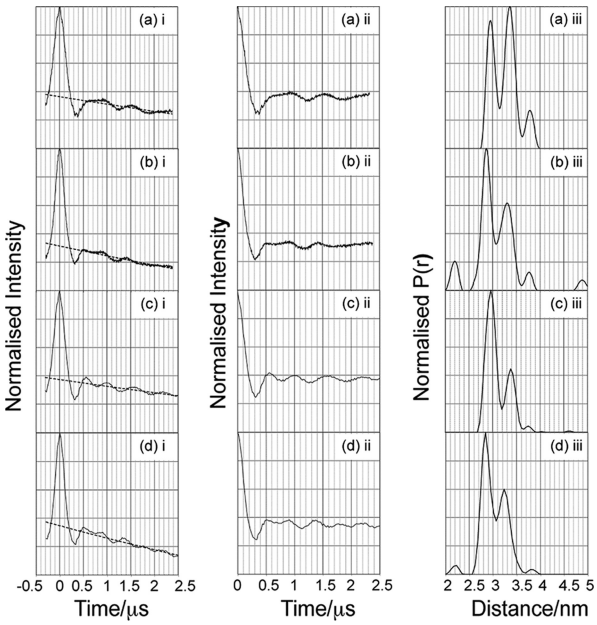

Figure 3. EPR data for endonuclease I T51R1 and the mutant K67A, with and without addition of DNA junction. (a) T51R1, (b) T51R1 plus DNA junction, (c) T51R1−K67A, (d) T51R1−K67A plus DNA junction. (i) Experimental PELDOR data with fitted baseline, indicated by dashed line. (ii) Background-corrected PELDOR data. (iii) Tikhonov-derived distance distribution. All data normalized for comparison. Absolute values are described in Table S1.

the structural effect of the K67A mutation might be transmitted indirectly to T51R1 via neighboring amino acids, bound metal ions, and the peptide backbone.

Distance Measurements on Spin-Labeled Endonuclease I, T51R1-K67A Junction Complex. When the T51R1-K67A construct was bound to a four-way DNA junction, there was very little change in the distance distribution from that seen with T51R1-K67A protein alone, except for a −1 Å shift in both major peaks (Figure 3(d)iii) as seen in the case of T51R1 bound to DNA junction (Figure 3(b)). Indeed, comparison of the distance distributions obtained from T51R1 and T51R1−K67A DNA junction complexes shows them to be almost identical (Figure 4(b)). This suggests that the K67A

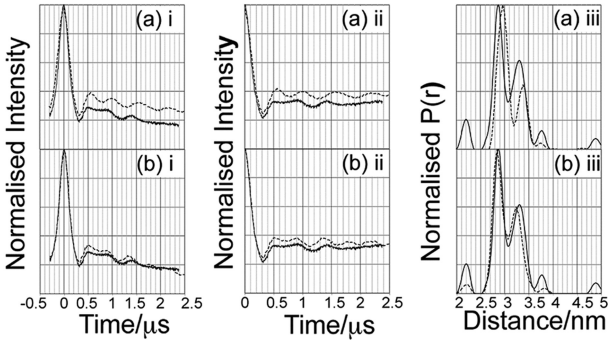

Figure 4. Effect of DNA binding on T51R1−K67A (a) T51R1 plus DNA junction (solid black line) compared with T51R1 K67A (dashed black line) and (b) T51R1 plus DNA junction (solid black line) compared with T51R1 K67A DNA junction (dashed black line). (i) Experimental PELDOR data. (ii) Background-corrected PELDOR data. (iii) Tikhonov-derived distance distribution.

mutation mimics the conformational change observed in endonuclease I upon DNA binding (Figure 4(a)).

Distance Measurements on Spin-Labeled Endonuclease I, T51R1: Summary. The EPR data show quite clearly that T51 exists in two states, whose ratio is influenced by both DNA binding and the K67A mutation in the active site. It appears that the K67A mutation affects the structure at T51 in a similar manner to that of DNA−4WJ. DNA binding causing a shift in distance distribution ratios and an additional overall −1 Å shift in both states.

Distance Measurements on Spin-Labeled Endonuclease I, S96C. To provide a comparison to the data derived from T51R1, a label site was chosen in a position almost diametrically opposed to T51, across the active site, at S96 (Figure 2). The raw data for S96R1 showed ∼1.5 clear oscillations (Figure 5(a)i,ii), and so a reasonably accurate

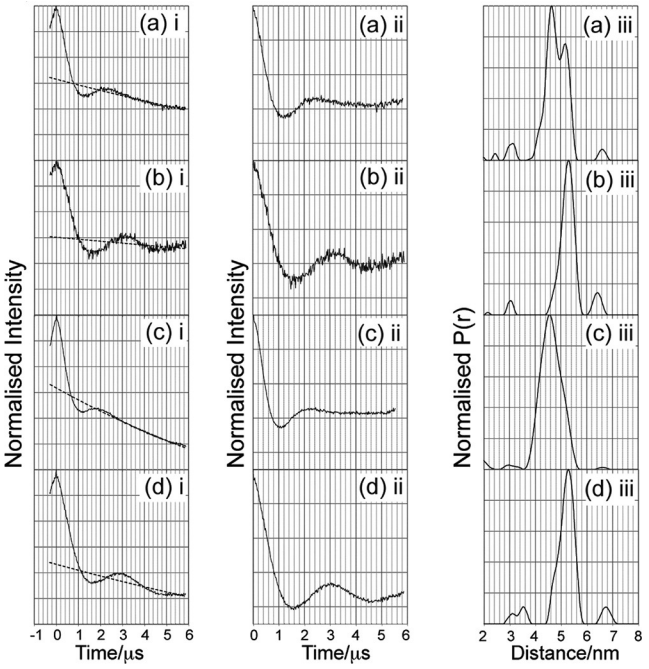

Figure 5. EPR data for endonuclease I S96R1 and the mutant K67A, with and without a DNA junction. (a) S96R1, (b) S96R1 plus DNA junction, (c) S96R1−K67A, (d) S96R1−K67A plus DNA junction. (i) Experimental PELDOR data with fitted baseline, indicated by dashed line, (ii) background-corrected PELDOR data, (iii) Tikhonov-derived distance distribution. All data have been normalized to the highest peak, for comparison. Absolute values are described in Table S1.

description of both the distance and the distance distribution between the spins was possible. There are fewer clear oscillations than seen for T51, so the distribution accuracy may be slightly reduced and there is an expectation of broader distributions. The distance distribution obtained from the Tikhonov regularization contained two major peaks (Figure 5(a)iii). The predominant peak is at 46 Å, and the minor peak is at 52 Å. Molecular dynamics from structure 1MO1 predicted a single distance of 46 Å, identical to the major distance distribution.

Distance Measurements on Spin-Labeled Endonuclease I S96R1−DNA Junction Complex. On binding a DNA junction to S96R1, the raw data showed just less than two oscillations (Figure 5(b)i,ii) and were collected for the same time as the S96R1 protein-alone data. The raw data show that

dx.doi.org/10.1021/bi2011898 | Biochemistry 2011, 50, 9963−9972

the frequency is lower, and the persistence of the oscillation has become slightly longer on binding a DNA junction. The resulting distance distribution has a predominant component at 53 Å (Figure 5(b)iii), which is comparable to the minor distance distribution that was present in S96R1 protein-alone (52 Å) (Figure 5(a)iii), and a shoulder at a slightly shorter distance. The observation of two distance distributions altering in ratio on binding to DNA is similar to the T51R1 data. The greater overlap in distance distributions makes determination of the ratio more difficult.

Distance Measurements on Spin-Labeled Endonuclease I, S96R1−K67A. We added the active site mutation K67A to endonuclease I S96R1 and studied the protein alone and in complex with DNA junction. The raw EPR data for S96R1−K67A show just over one oscillation (Figure 5(c)i,ii), very similar to those for S96R1 as protein alone. The derived distance distribution (Figure 5(c)iii) is closely similar to that for S96R1, with a predominant peak at 46 Å and a minor peak at 52 Å.

Distance Measurements on Spin-Labeled Endonuclease I, S96R1−K67A Junction Complex. The raw data show almost two complete oscillations (Figure 5(d)i,ii), nearly identical to those observed in S96R1 bound to DNA (Figure 5(b)i,ii), and the derived distance distribution is also clearly very similar to S96R1 DNA junction complex, with a predominant peak at 52.7 Å and a width at half-height of 6.3 Å. Therefore, we observe a shift to the longer distance in the K67A mutant of S96R1 upon binding DNA junction. A slight shoulder in the main distance distribution is also similar to that seen for the unmutated protein in complex with DNA

Distance Measurements on Spin-Labeled Endonuclease I, S96R1: Summary. The EPR data suggest that position S96 is sensitive to structural changes in endonuclease I that occur upon binding of the DNA junction but relatively insensitive to the changes made by the mutation of an active site residue. The observations on the effect of K67A contrast with those for position T51, but S96 is situated within the globular domain of endonuclease I and on the opposite face of the protein from T51.

Distance measurements on spin-labeled endonuclease I K22C. In order to provide further data on the overall protein conformation and in particular to investigate the nature of the α1 N-terminal helix, a label site was introduced at position K22. The raw data for K22R1 show just over one clear oscillation (Figure 6(a)i,ii), and therefore an accurate description of the distance was possible. The distance distribution obtained shows one predominant peak at 65 Å and a shoulder at just under 60 Å (Figure 6(a)iii). Interestingly, in the case of K22R1 molecular dynamics predicts a shorter set of distances, with the modal value being at 59 Å (6 Å shorter than that observed experimentally). Given that for the other positions studied modal distances have agreed very well with the EPR determined distances, this suggests that K22R1 adopts a position that is slightly different from that observed in the crystal structure (1MOI).

Distance Measurements on Spin-Labeled Endonuclease I, K22R1 Junction Complex. The raw data have been collected over the same time as K22R1. By comparison, it can be seen that there is a very small but discernible shift to a shorter frequency (Figure 6(b)i,ii). The resulting distance distribution has a slightly shorter, predominant distance peak, at 62 Å but also a shoulder at just over 65 Å (Figure 6(b)iii). Comparison of the distance distributions, with and without

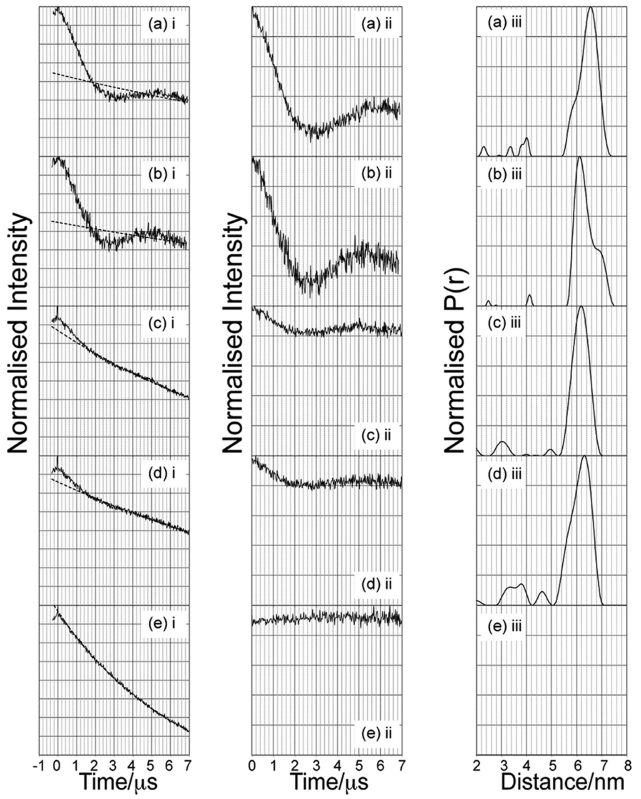

Figure 6. EPR data for endonuclease I K22R1 and the mutant K67A, with and without junction DNA. (a) K22R1, (b) K22R1 plus junction DNA, (c) K22R1−K67A, (d) K22R1−K67A plus junction DNA, (e) K22R1 D55A. (i) Experimental PELDOR data with fitted baseline, indicated by dashed line. (ii) Background-corrected PELDOR data. (iii) Tikhonov-derived distance distribution. All data have been normalized for comparison. Absolute values are described in Table S1.

DNA, suggests strongly that there is a significant shift in the ratios of the components of the distance distribution, similar to the observed for the other two label sites.

Distance Measurements on Spin-Labeled Endonuclease I K22R1−K67A. The raw EPR data for K22R1−K67A are composed predominantly of a decaying signal (Figure 6(c)i,ii), which, after background correction (assuming homogeneous 3D background) yields a dipolar oscillation that has a far shallower modulation depth than observed in data for the K22R1 protein lacking the active site mutation. The resultant distance distribution shows a peak at 62 Å (Figure 6(c)iii). The predominant distance is the same as shown by K22R1 when bound to DNA junction.

The observed low modulation depth could have a number of explanations. Mass spectrometry revealed a predominant peak at the expected mass for endonuclease I with attached spin-label, so ruling out a low extent of labeling and thus a high proportion of singly labeled dimer. Another possible explanation could be that the majority of the endonuclease I was no longer a dimer. However, since it is possible to observe a dipolar oscillation from K22R1-wt and from other spin-labeling sites with the K67A mutation, it would suggest that neither the K22R1 or K67A mutations affect the dimerization of endonuclease I. Another possibility is that the α1-helix is no longer situated next to the globular domain of endonuclease I in a major fraction of the sample, possibly having become largely unstructured. Spin-label attached to unstructured α1-

Table 1. Comparison between Distances (in Å) Using EPR and Those Derived from Modeling Spin-Label Positions onto Crystal Structures

position[a]	1MOI (noDNA)[b]	EPR (noDNA)[c]	diff (noDNA)[d]	2PFJ (DNA)[e]	EPR (DNA)[f]	diff (DNA)[g]	Xtal diff[h]	EPR diff[i]
T51	33.5	33.0	−0.5	30.0	29.0	−1.0	−4.5	−4.0
S96	45.0	45.0	0.0	48.3	52.0	3.7	3.3	6.0
K22	59.0	64.0	5.0	54.0	60.0	6.0	−5.0	−4.0

[a]Locations of the spin-labels. [b]Distances calculated from crystal structure of endonuclease I in the absence of a DNA junction 1MOI. [c]PELDOR-derived distances in endonuclease I without bound DNA. [d]Difference between distances taken from crystal structure with DNA (1MOI) and the PELDOR-derived distances. [e]Distances taken from the DNA junction-bound crystal structure 2PFJ. [f]PELDOR-derived distance from endonuclease I with bound DNA junction. [g]Difference between distances taken from crystal structure without DNA (2PFJ) and the PELDOR-derived distances. [h]Distance difference upon DNA binding, derived from crystal structures. [i]Distance difference upon DNA binding, calculated from PELDOR data.

helix could result in these spins resembling the background, that is, spins that are homogeneously distributed in solution and whose contribution to the PELDOR signal is estimated by fitting of a homogeneous 3D model of intermolecular spin interactions.

Distance Measurements on Spin-Labeled Endonuclease I K22R1−K67A Junction Complex. The raw EPR data for K22R1−K67A bound to the DNA junction (Figure 6(d)i,ii) show a decaying signal that is almost identical to that observed for the same protein without DNA. After background correction a very weak modulation was observed that gives rise to a distance peak at 63 Å by Tikhonov regularization (Figure 6(d)iii). These data suggest that even when bound to a four-way DNA junction, a large proportion of the α1-helix of endonuclease I K67A is unstructured, and so the majority of the spin-label, K22R1, has the characteristic of normal background intermolecular coupling. This indicates that the presence of the DNA is not sufficient to stabilize the α1-helix when the active site contains the K67A substitution.

The α1-helix is held in place by a combination of interactions with the globular domain of endonuclease I. It can be seen from the crystal structure of endonuclease I (1M0D) that L19, V23, and L27, on the α1-helix, are directed into a hydrophobic pocket comprising F34 and Y36 of the same polypeptide and F56, V64, V93, and I125 from the other polypeptide of endonuclease I. The location of the α1-helix is also likely to be stabilized by the interaction of E20 with one of the two metal ions that bind at the active site[26] (Figure 2(a)). The K67A mutation is known to reduce the number of metal ions bound at the active site to one (Déclais and Lilley, unpublished data). If the metal ion to be lost were that interacting with E20, this could be the origin of the destabilization of the α1-helix. This destabilization may be compounded by the influence of the other two negatively charged side chains (D55 and E65) that are directed into the active site, which may have the effect of repelling E20, and the α1-helix, from its stable location.

Distance Measurements on Spin-Labeled Endonuclease I K22R1−D55A. To test the effect of active site disruption further, the effect of the D55A mutation on K22R1 was measured (Figure 6(e)). Addition of the D55A mutation led to further destabilization of the α1-helix, resulting in data that were indistinguishable from intermolecular background. No trace of an intramolecular dipolar-derived oscillation could be discerned in the data. A control experiment studying S96R1 in the presence of the D55A mutation (data not shown) demonstrated that the endonuclease I dimer was globally intact, and good labeling efficiency was also confirmed. We conclude that mutations that destabilize the active site can result in loss of α1-helix integrity.

Distance Measurements on Spin-Labeled Endonuclease I K22R1: Summary. The results obtained for K22R1 indicate that, in the absence of active site mutation, the α1-helix exists in two conformations, neither of which conform, absolutely, to that observed in the crystal structures. Binding to a DNA junction results in a change in the ratio of the two conformers, in a manner similar to that observed for T51R1. The active site mutation K67A, which affected the conformer ratio in T51, also has an effect on the conformer ratios monitored by K22R1. Furthermore, mutation K67A has a large effect in destabilizing the α1-helix. D55A mutation had an even more pronounced effect on the stability of the α1-helix; this side chain is probably directly coordinated to both active site metal ions and is likely to have a more direct impact on the structural integrity of the active site.

Using simple molecular dynamics to model spin-label distributions on the crystal structures 1MOI (no bound DNA) and 2PFJ (complex with DNA junction) provided estimates of both distances and distance distributions for the two forms (shown graphically in Figure S10a−c). Comparison of these modeled distances with the distances derived from Tikhonov regularization applied to the PELDOR data led to the values tabulated in Table 1. The experimental PELDOR-derived distances were taken from the two major peaks that were present in most of the data, based on the assumption that the shift in ratio observed upon binding DNA corresponded to a change from the nonbound to the bound state. The binding of a DNA junction to endonuclease I leads to decreased distances for T51R1 and K22R1 and an increase for S96R1, seen both in the crystal structures and the PELDOR results (Table 1, columns *h* and *i*). The absolute values of the distance difference in going from free to DNA bound forms are closely comparable for positions T51 and K22 but diverge considerably in the case of position S96. The absolute distances estimated from the crystal structures compared to the PELDOR-derived distances are in reasonable agreement for positions T51 and S96, but K22 presents a greater discrepancy.

Activity of Mutant and Spin-Labeled Mutant Endonuclease I. In general, the mutant forms of T7 endonuclease I bind DNA four-way junctions with a slightly higher affinity. Derivitization of the cysteine mutants, with MTSSL, slightly reduces the affinity of endonuclease I for the junction, in most cases. In all cases binding remains tight with a favorable comparison to endonuclease I wild-type affinity. Results are shown in Supporting Information Table 2.

All active cysteine mutants (not K67A mutants) cleave the junction efficiently at the same position as the wild-type endonuclease I, resulting in the observation of a 14 base DNA strand.

The mutation K67A in endonuclease I reduces, by at least 10000 times, the catalytic activity of the protein. The cysteine mutants and their MTSSL derivatives behave similarly. A slight rescue in the catalytic activity by endonuclease I K22C K67A and its MTSSL derivative can be seen, but the activity remains extremely low compared to the non-K67A protein. Images of the polyacrylamide gels showing radio-labeled junction cleavage are shown in Supporting Information Figure S10.

DISCUSSION

In this study we have used electron paramagnetic resonance to report on the distances between three selected amino acid positions, in the two polypeptides of the endonuclease I enzyme, free and in complex with a DNA junction. The vector connecting residues at position 51 (T51R1) pass along the β-bridge between the two domains of the dimer, and the T51 side chains are close to the continuous strands of the DNA in the complex, crossing the major groove side of the junction. The other two vectors traverse the minor groove side of the junction in the complex. One (position 96: S96R1) connects amino acids in the main body of each domain, while the other (position 22: K22R1) connects the two N-terminal α-helices that originate from the remote domains of the dimer.

The EPR data we have collected on the endonuclease I system are of exceptionally high quality, permitting us to interpret the distance distributions with good confidence. The accuracy of both distance and, more critically, distance distributions derived from PELDOR data depend on the noise level, the accuracy of background estimation, and, most importantly, the persistence of the signal oscillations. For accurate determination of both distance and distribution, the observation of at least one full oscillation is required, and the accuracy improves with the measurement of further oscillations.[16] For T51R1 we have observed more than 4 complete oscillations, nearly 3 for S96R1, and in the case of K22R1 with distances greater than 60 Å we have measured about 1.5 complete oscillations. Calculated L curves (parametric plots that compare smoothness of the distance distribution to the mean square deviation—see Supporting Information) are generally excellent, giving an unambiguous choice of regularization factor, alpha. Some of the most important observations in this work arise from the observation of the changing ratios of two very close distance distributions. It is the fundamental quality of the data that makes these comparisons legitimate.

The PELDOR data obtained from the three vectors indicate that there are at least two conformations of endonuclease I as a free dimer. For example, there are two major peaks observed in the distance distribution calculated for the protein with spin-labels attached at position 51. In past work we have found that two alternative complexes analogous to the alternative stacking conformers of the free junction exist.[27] However, that is not the origin of these species because we have studied a cruciform junction with two short arms that completely forces the complex into a single form.[9] For the T51R1 species the difference between the major peaks is 4 Å, suggesting a small but significant difference in conformation. Distances between spin-labels measured for the major form are in good agreement with those deduced from the crystallographic structure for the T51R1 and S96R1 vectors (Table 1).

Differences in the crystal structures of endonuclease I free[10] and bound to a DNA junction[12] suggest that DNA binding is accompanied by a small reorganization of the protein structure, and we observed that the distance distributions did indeed change on binding. In general, we observe the same bimodal distribution of distances for each of the three spin-label pairs, but what was the minor peak in the free protein becomes the major peak in the complex with the DNA junction for each vector. This suggests that binding to the DNA junction stabilizes the minor conformation that exists in the population of free enzyme in an induced-fit process. However, interpretation of the changes in terms of a simple two-state process is likely to be an oversimplification, since the data indicate that the population of the DNA-bound forms remains bimodal.

In switching between the two conformations the distances change by $\leq$6 Å, and both the magnitude and direction of the changes are in good agreement with those deduced from the two crystal structures. For example the EPR data indicate that the T51R1 distance for the free protein of 33.5 Å shortens by 3.5 Å on binding to the junction; modeling spin-label positions onto the crystal structures suggests that a distance of 33.0 Å shortens by 4.0 Å. By contrast, the distance between labels on S96R1 (45.0 Å calculated from both crystallographic and EPR data) lengthens by 3.3 and 6.0 Å on binding DNA deduced from EPR and crystallography, respectively. Thus, changes in distance in opposite senses are consistently reproduced by the two approaches, indicating that the conformational change observed in the crystal also occurs in solution.

When endonuclease I binds to a DNA junction, there is an intimate interaction between the components of the active sites and the DNA.[14,9,12] Each active site contains two divalent metal ions that are coordinated by the carboxylate side chains of aspartate 55 and glutamate 65 and the *pro*S nonbridging oxygen atom of the scissile phosphate, and mutation of these residues significantly impairs both activity[26,28] and metal ion binding.[14] Glutamate 20 (contributed by the other polypeptide of the dimer) and lysine 67 also play important roles in the active center, and substitution of any of the four side chains significantly impairs enzyme activity. Interestingly, we have observed that substitution of the active site lysine (K67A) has a marked effect on the distance distributions observed for the T51R1 and K22R1 vectors, in a manner very similar to those resulting from DNA binding. Thus, the substitution (perhaps the loss of positive charge) appears to mimic the effect of binding a DNA junction, apparently stabilizing the free enzyme in a conformation resembling the DNA-bound state. However, a corresponding effect is not observed for the S96R1 vector, reinforcing the view that the conformational changes are more complex than a simple two-state hinge motion.

The K22R1 vector has a special significance because the spin-label is attached to the N-terminal α-helix. The N-terminal amino acids of endonuclease I (i.e., the section immediately preceding this helix) are not visible in the crystal structures of either the free protein or its complex with a DNA junction, suggesting that it is disordered in the crystal. N-terminal deletions of endonuclease I have markedly altered junction binding properties (unpublished). While the coupling between the labels attached at position 22 is clearly detectable for the wild-type sequence enzyme, when additional mutations were introduced into the active site, this became less pronounced (K67A) or absent (D55A), indicating either a displacement or disordering of the helix. This demonstrates that there is a strong connection between the active site and the N-terminal α-helix.

All biophysical techniques suffer from some conditional bias leading to the possibility of artifactual observation. The

combination of data from crystallography and EPR, as presented here, lends confidence to the structural conclusions and broadens our understanding of the structure−function relationship. In the binding of endonuclease I to its cruciform DNA target, gross changes to the DNA structure are observed. The protein dimer itself exhibits more subtle changes in conformation, which are strongly implicated in the precise mode of enzyme action.

■ ASSOCIATED CONTENT

Supporting Information

Additional figures showing labeling strategy for both DNA and protein; figures showing L curves corresponding to main PELDOR data, goodness of fit (of Tikhonov) to background corrected PELDOR data, additional PELDOR data for E83R1 D55A, distance distributions derived from crystal structure 1MOI, a table of EPR data collection parameters, a table showing binding measurements, and a figure showing junction cleavage activity, for mutant and MTSSL derivatized proteins. This material is available free of charge via the Internet at http://pubs.acs.org.

■ AUTHOR INFORMATION

Corresponding Author

*E-mail: d.g.norman@dundee.ac.uk. Phone +44(0)1382 384798. Fax +44(0)1382 386373.

Author Contributions

[§]The first two authors contributed equally to this work.

Funding

This work was funded by The Engineering and Physical Sciences Research Council (EP/F0390341) and Cancer Research UK.

■ ACKNOWLEDGMENTS

We thank David Keeble (Dundee), Graham Smith, Olav Schiemann (St. Andrews), and Simon Phillips (Harwell) for discussion and Scott McPhee for expert DNA synthesis.

■ REFERENCES

(1) Holliday, R. (1964) A mechanism for gene conversion in fungi. *Genet. Res. 5*, 282−304.

(2) Potter, H., and Dressler, D. (1976) On the mechanism of genetic recombination: electron microscopic observation of recombination intermediates. *Proc. Natl. Acad. Sci. U. S. A. 73*, 3000−3004.

(3) Orr-Weaver, T. L., Szostak, J. W., and Rothstein, R. J. (1981) Yeast transformation: a model system for the study of recombination. *Proc. Natl. Acad. Sci. U. S. A. 78*, 6354−6358.

(4) Schwacha, A., and Kleckner, N. (1995) Identification of double Holliday junctions as intermediates in meiotic recombination. *Cell 83*, 783−791.

(5) White, M. F., Giraud Panis, M. J. E., Pöhler, J. R. G., and Lilley, D. M. J. (1997) Recognition and manipulation of branched DNA structure by junction-resolving enzymes. *J. Mol. Biol. 269*, 647−664.

(6) Center, M. S., and Richards, C. C. (1970) Endonuclease Induced after Infection of Escherichia-Coli with Bacteriophage-T7 II. Specificity of Enzyme toward Single- and Double-Stranded Deoxyribo-Nucleic Acid. *J. Biol. Chem. 245*, 6292−6299.

(7) Sadowski, P. D., Warner, H. R., Hercules, K., Munro, J. L., Mendelso., S., and Wiberg, J. S. (1971) Mutants of Bacteriophage T4 Defective in Induction of T4 Endonuclease I. *J. Biol. Chem. 246*, 3431−3433.

(8) Davanloo, P., Rosenberg, A. H., Dunn, J. J., and Studier, F. W. (1984) Cloning and Expression of the Gene for Bacteriophage-T7 RNA-Polymerase. *Proc. Natl. Acad. Sci. U. S. A. 81*, 2035−2039.

(9) Déclais, A. C., Liu, J., Freeman, A. D. J., and Lilley, D. M. J. (2006) Structural recognition between a four-way DNA junction and a resolving enzyme. *J. Mol. Biol. 359*, 1261−1276.

(10) Hadden, J. M., Convery, M. A., Déclais, A. C., Lilley, D. M., and Phillips, S. E. (2001) Crystal structure of the Holliday junction resolving enzyme T7 endonuclease I. *Nat. Struct. Biol. 8*, 62−67.

(11) Hadden, J. M., Déclais, A. C., Phillips, S. E., and Lilley, D. M. (2002) Metal ions bound at the active site of the junction-resolving enzyme T7 endonuclease I. *EMBO J. 21*, 3505−3515.

(12) Hadden, J. M., Déclais, A. C., Carr, S. B., Lilley, D. M., and Phillips, S. E. (2007) The structural basis of Holliday junction resolution by T7 endonuclease I. *Nature 449*, 621−624.

(13) Parkinson, M. J., and Lilley, D. M. J. (1997) The junction-resolving enzyme T7 endonuclease 1. Quaternary structure and interaction with DNA. *J. Mol. Biol. 270*, 169−178.

(14) Freeman, A. D. J., Déclais, A. C., and Lilley, D. M. J. (2003) Metal ion binding in the active site of the junction-resolving enzyme T7 endonuclease I in the presence and in the absence of DNA. *J. Mol. Biol. 333*, 59−73.

(15) Todd, A. P., Cong, J. P., Levinthal, F., Levinthal, C., and Hubbell, W. L. (1989) Site-Directed Mutagenesis of Colicin-E1 Provides Specific Attachment Sites for Spin Labels Whose Spectra Are Sensitive to Local Conformation. *Proteins: Struct., Funct., Genet. 6*, 294−305.

(16) Jeschke, G., Koch, A., Jonas, U., and Godt, A. (2002) Direct conversion of EPR dipolar time evolution data to distance distributions. *J. Magn. Reson. 155*, 72−82.

(17) Martin, R. E., Pannier, M., Diederich, F., Gramlich, V., Hubrich, M., and Spiess, H. W. (1998) Determination of end-to-end distances in a series of TEMPO diradicals of up to 2.8 nm length with a new four-pulse double electron electron resonance experiment. *Angew. Chem., Int. Ed. 37*, 2834−2837.

(18) Milov, A. D., Salikohov, K. M., and Shchirov, M. D. (1981) Use of the double resonance in electron spin echo method for the study of paramagnetic center spatial distribution in solids. *Fizika Tverdogo Tela 23*, 975−982.

(19) Pannier, M., Veit, S., Godt, A., Jeschke, G., and Spiess, H. W. (2000) Dead-Time Free Measurement of Dipole-Dipole Interactions between Electron Spins. *J. Magn. Reson. 142*, 331−340.

(20) Schiemann, O., and Prisner, T. F. (2007) Long-range distance determinations in biomacromolecules by EPR spectroscopy. *Q. Rev. Biophys. 40*, 1−53.

(21) Richard, W., Bowman, A., Sozudogru, E., El-Mkami, H., Owen-Hughes, T., and Norman, D. G. (2010) EPR distance measurements in deuterated proteins. *J. Magn. Reson. 207*, 164−167.

(22) Ward, R., Bowman, A., El-Mkami, H., Owen-Hughes, T., and Norman, D. G. (2009) Long Distance PELDOR Measurements on the Histone Core Particle. *J. Am. Chem. Soc. 131*, 1348−1349.

(23) McKinneyS. A.DéclaisA. C.LilleyD. M. J.HaT. (2003) 2003Structural dynamics of individual Holliday junctionsNature Struct. Biol.

(24) DeLano, W. L. (2002). *The PyMOL Molecular Graphics System*, DeLano Scientific, Palo Alto, CA.

(25) Polyhach, Y., Bordignon, E., and Jeschke, G. (2011) Rotamer libraries of spin labelled cysteines for protein studies. *Phys. Chem. Chem. Phys. 13*, 2356−2366.

(26) Déclais, A. C., Hadden, J., Phillips, S. E., and Lilley, D. M. (2001) The active site of the junction-resolving enzyme T7 endonuclease I. *J. Mol. Biol. 307*, 1145−1158.

(27) Déclais, A. C., Fogg, J. M., Freeman, A. D. J., Coste, F., Hadden, J. M., Phillips, S. E. V., and Lilley, D. M. J. (2003) The complex between a four-way DNA junction and T7 endonuclease I. *EMBO J. 22*, 1398−1409.

(28) Liu, J., Déclais, A. C., and Lilley, D. M. J. (2006) Mechanistic aspects of the DNA junction-resolving enzyme T7 endonuclease I. *Biochemistry 45*, 3934−3942.

(29) Beaucage, S. L., and Caruthers, M. H. (1981) Deoxynucleoside Phosphoramidites - a New Class of Key Intermediates for Deoxypolynucleotide Synthesis. *Tetrahedron Lett. 22*, 1859−1862.

(30) Sinha, N. D., Biernat, J., Mcmanus, J., and Koster, H. (1984) Polymer Support Oligonucleotide Synthesis XVIII: Use of Beta-Cyanoethyl-N,N-Dialkylamino-/N-Morpholino Phosphoramidite of Deoxynucleosides for the Synthesis of DNA Fragments Simplifying Deprotection and Isolation of the Final Product. *Nucleic Acids Res. 12*, 4539−4557.

(31) Edwards, T. E., Okonogi, T. M., Robinson, B. H., and Sigurdsson, S. T. (2001) Site-specific incorporation of nitroxide spin-labels into internal sites of the TAR RNA; structure-dependent dynamics of RNA by EPR spectroscopy. *J. Am. Chem. Soc. 123*, 1527−1528.

(32) Edwards, T. E., Okonogi, T. M., and Sigurdsson, S. T. (2002) Investigation of RNA-protein and RNA-metal ion interactions by electron paramagnetic resonance spectroscopy: The HIV TAR-Tat motif. *Chem. Biol. 9*, 699−706.

(33) Jeschke, G., Chechik, V., Ionita, P., Godt, A., Zimmermann, H., Banham, J., Timmel, C. R., Hilger, D., and Jung, H. (2006) DeerAnalysis2006 - a comprehensive software package for analyzing pulsed ELDOR data. *Appl. Magn. Reson. 30*, 473−498.

(34) Schwieters, C. D., Kuszewski, J. J., Tjandra, N., and Clore, G. M. (2003) The Xplor-NIH NMR molecular structure determination package. *J. Magn. Reson. 160*, 65−73.

(35) Bowman, A., Ward, R., El-Mkami, H., Owen-Hughes, T., and Norman, D. G. (2010) Probing the (H3-H4)2 histone tetramer structure using pulsed EPR spectroscopy combined with site-directed spin labelling. *Nucleic Acids Res. 38*, 695−707.